Hot electrons in the interaction of femtosecond laser pulses with foil targets at a moderate laser intensity

Y. T. Li,[1,2] J. Zhang,[1,*] L. M. Chen,[1,2] Y. F. Mu,[2] T. J. Liang,[3] Z. Y. Wei,[1] Q. L. Dong,[1] Z. L. Chen,[1] H. Teng,[1] S. T. Chun-Yu,[2] W. M. Jiang,[2] Z. J. Zheng,[2] and X. W. Tang[3]

[1]*Laboratory of Optical Physics, Institute of Physics, Chinese Academy of Sciences, Beijing 100080 , Peoples Republic of China*

[2]*National Key Laboratory for Laser Fusion, Institute of Nuclear Physics and Chemistry, China Academy of Engineering Physics, Mianyang 621900, Peoples Republic of China*

[3]*Institute of High Energy Physics, Chinese Academy of Sciences, Beijing 100039, People's Republic of China*

(Received 6 December 2000; revised manuscript received 9 April 2001; published 26 September 2001)

Characteristics of hot electrons produced in the interaction of femtosecond laser pulses with foil targets were investigated at a moderate laser intensity. Both outgoing and ingoing hot electrons from the femtosecond laser plasma were studied. A collimated jet of outgoing hot electrons was observed in the target normal direction. An ingoing energetic hot-electron beam was found in the laser propagation direction, while the low-energy ingoing electrons spread into wider cone angle due to the collisional effects in the plasma and target material. These observations were supported by three-dimensional Monte Carlo simulations. The hot-electron temperature obtained from electron spectra and absorption experiments implies that resonance absorption is partially responsible for the generation of hot electrons.

DOI: 10.1103/PhysRevE.64.046407 PACS number(s): 52.25.Os, 52.38.−r

I. INTRODUCTION

The rapid development of short pulse ultraintense lasers provides powerful tools to study relativistic laser-plasma interactions and explore approaches to ignition of inertial confinement fusion. For example, the fast ignition concept proposed by M. Tabak *et al*. is one of the most promising ways [1]. One of the major physics issues to implement fast ignition is the generation and propagation of energetic hot electrons in high-density plasmas. Recently, the energetic hot electrons outgoing from plasmas were studied experimentally and theoretically [2–7]. Hot-electron energies up to 100 MeV were observed in laser-solid interactions at an intensity of 3×10^{20} W/cm^2 using petawatt laser system at LLNL [8]. G. Malka and J. L. Miquel also studied relativistic electrons produced by interaction of relativistically intense laser pulses with solid targets [9]. The high energy of hot electrons was attributed to $\mathbf{J}\times\mathbf{B}$ acceleration mechanism [10]. On the other hand, hot electrons ingoing along the laser propagation direction, which is directly related with fast ignition, were also studied in detail [11,12]. M. Tatarakis *et al.* observed a plasma at the back surface of a thin foil. This was believed to be formed by a collimated electron beam passing through the foil [13]. A more direct experiment was carried out using a transparent glass target coated with an aluminum layer. An ionization track induced by a beam of energetic hot electrons was clearly observed through the target [14,15]. P. A. Norreys *et al*. observed a highly directional γ-ray beam with energies above 10 MeV in the direction nearly opposite to the target normal direction. This indicated the generation of a directional relativistic electron beam [16]. These experimental results imply that the hot-electrons could be collimated by self-generated magnetic fields. The generation of hot-electron jet and the pinching of magnetic fields were reproduced by particle-in-cell (PIC) simulations [17,18].

Many mechanisms can produce hot electrons. In the interaction of intense laser pulses with sharp solid-vacuum interface, the ponderomotive potential model and Brunel absorption model [19] play important roles. Other mechanisms such as wake fields [20], parametric instabilities [21,22], B-loop mechanism [23], and propagating wave [24] are effective when a large-scale preplasma is formed before the arrival of the main laser beam.

In this paper, we show that the well-collimated emission of hot electrons is not only generated at relativistic laser intensities, but also at a moderate laser intensity. The angular distribution of the outgoing and ingoing hot electrons, the electron energy spectrum, the generation mechanism, and the transport of hot electrons into cold target material are investigated in interaction of femtosecond laser pulses with foil targets.

II. EXPERIMENTAL SETUP

The experiments were carried out with a Ti:Sapphire laser system at the Institute of Physics, Chinese Academy of Sciences. The laser has a 5 mJ output energy in 150 fs pulses at 796 nm. A *p*-polarized laser beam was focused by an $f/5$ lens onto foil targets with an average intensity of 5×10^{15} W/cm^2. The target was moved 0.5 mm per second so that the laser pulses interacted with a fresh target surface for every shot. For some shots, a prepulse with 8% energy of the main laser pulse was applied to create a preplasma with which the main laser pulse interacted after a 50-ps delay time.

Figure 1 shows the experimental layout. In the first part of the experiments, the laser beam was focused onto a 100-μm-thick aluminum foil at 45° to the target normal. A six-channel electron spectrometer with 380 G permanent magnets was set in the normal direction to measure the electron energy distribution in the range of 7–500 keV [25]. LiF detectors were used. Radiochromic films with aluminum fil-

*Author to whom correspondence should be addressed. Email address: jzhang@aphy.iphy.ac.cn

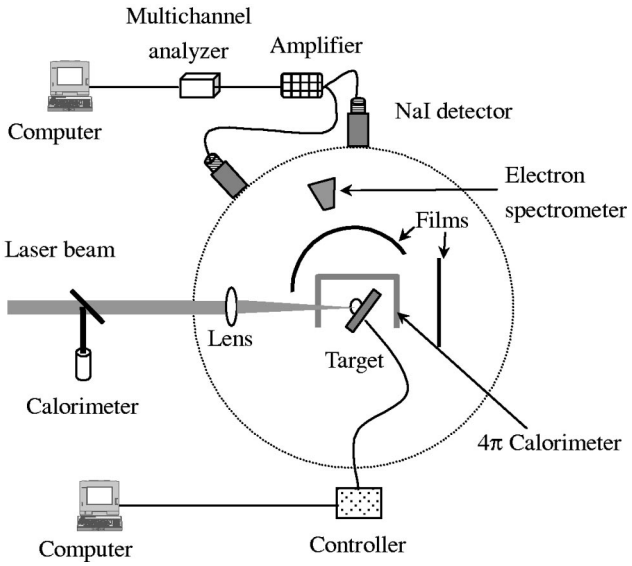

FIG. 1. Schematic of experimental setup. A 4π calorimeter was used to measure the energy absorption. The laser energy was monitored by the calorimeter outside the target chamber. The energy distribution and the spatial distribution of hot electrons ejected from the plasma were detected by an electron spectrometer and radiochromic films surrounding the plasma, respectively. The NaI system was used to monitor the intensity of x-ray emission, which provided information on focal quality.

ters, surrounding the plasma generated by the laser beam, recorded the outgoing hot electrons escaping from the plasma at the front side of the target. A 4π calorimeter measured the laser energy absorption. A 2-mm-thick quartz cylinder inside the calorimeter blocked charged particles and x-ray emission. In order to study the ingoing hot electrons, in the second part of experiments, 5-μm thin foil targets were used. The ingoing energetic hot electrons along the laser propagation direction, after passing through the thin foil, were recorded by a radiochromic film at the backside of the target. The incident angle was chosen to be 30°, because the energy absorption measurement showed a higher coupling efficiency at 30° incidence angle. The NaI detective system shown in Fig. 1 was used to measure the x-ray emission [26]. This system has become our routine diagnostic not only to study the hard x-ray emission, but also to monitor the focal condition.

III. RESULTS AND DISCUSSION

A. Thick foil experiments

1. Angular distribution of backward hot electrons

We used an aluminum filter assembly in front of the radiochromic film to select the desirable electron energy range. The radiochromic film recorded the electrons, ions, and x-rays passing through the filter assembly. However, the sensitivity of the film to charged particles is higher than that to photons. Previous ion measurements using CR-39 showed that the maximum proton energy produced under the same conditions was less than 500 keV [27], whose penetration depth was about 4 μm in aluminum material. Therefore the ion contribution to the film exposure is negligible because the thickness of the aluminum filter used in our experiments was at least larger than 8 μm. To check the effects of x-rays on the film exposure, a calibration experiment was performed. Two permanent magnets were employed to remove the electrons with energies less than 500 keV (see Fig. 3). Comparison of the exposure value of the film for the conditions with and without external magnetic field showed that the contribution of x rays was two-orders magnitude lower than that of hot electrons. This comparison ensured us that the exposure of the film was mainly caused by hot electrons.

Figure 2 shows the angular distribution of outgoing hot electrons with energies greater than 50 keV in the incident plane. The electrons were generated by *p*-polarized laser irradiation at a 45° incidence angle with a prepulse 50 ps before the main beam. The solid line in Fig. 2(a) is a microdensitometer trace of angular distribution of hot electrons produced from a 100-μm-thick aluminum foil. The dotted line is a Gaussian fit. Each data point here represents an average of 30 shots. 0° on the *x* axis corresponds to the backward direction of the laser beam. We can see that the outgoing electrons escaped from the plasma in the target normal direction were well collimated.

The collimated electron jets observed here are very similar to the theoretical prediction obtained by H. Ruhl *et al.* [17] and Y. Sentoku *et al.* [18] using PIC and Vlasov simu-

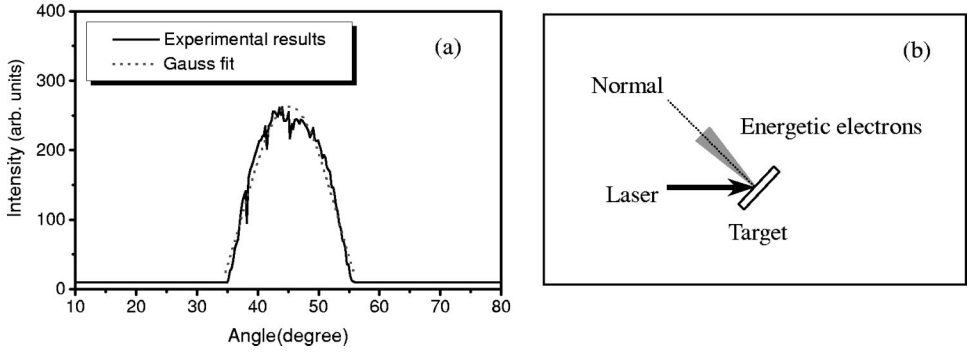

FIG. 2. (a) The angular distribution of outgoing hot electrons with energies over 50 keV in the incident plane. The electrons were generated by *p*-polarized irradiation at 45° incidence with a prepulse 50 ps before the main beam. The laser intensity was 5×10^{15} W/cm^2. The peak located at the normal direction (45°). (b) Sketch of the outgoing energetic electron emission in front of the target.

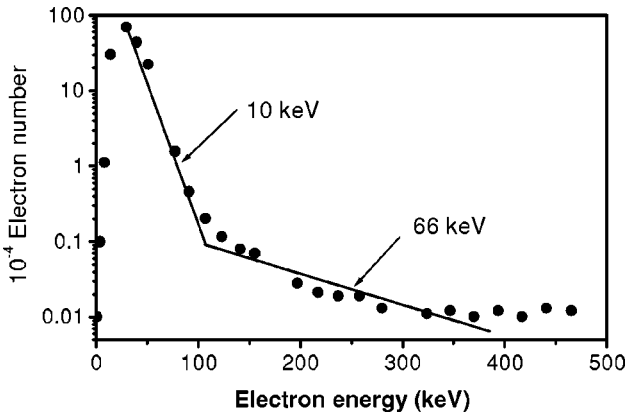

FIG. 3. Typical energy spectrum of outgoing hot electrons measured in the normal direction produced in the laser-thick foil target experiments. The foil was irradiated by *p*-polarized laser at 45° incidence with a prepulse of 50 ps separation time with the main beam. The laser intensity was 5×10^{15} W/cm^2. The two hot-electron temperatures were obtained from exponential fit to the experimental data.

lations. They found electron jets in the interaction of *p*-polarized laser irradiation incident at 30° and 45° on a fully ionized target with an underdense preplasma corona. The self-generated magnetic fields occurred simultaneously and collimated the energetic hot electrons. A scaling law of the outgoing angle of the hot electrons determined by lateral canonical momentum conservation in boost frame coordinates was proposed as

$$\theta' = \tan^{-1}\left[\frac{\sqrt{1+\alpha I\lambda^2/10^{18}}-1}{\sqrt{\alpha I\lambda^2/10^{18}}}\tan\theta\right], \qquad (1)$$

where θ' is the electron emission angle to the target normal, θ is the laser incident angle, $I\lambda^2$ is the laser intensity in W cm^{-2} μm^2, and α relates the mean longitudinal momentum to the laser intensity. Two simulations were made by H. Ruhl using PIC and Vlasov simulations for nonrelativistic intensities and for relativistic intensities, respectively. Substituting the simulation parameters used by the authors into Eq. (12) in Ref. [17], one can obtain $\alpha=2.8\times10^{-18}$ W^{-1} cm^2 μm^{-2} for the case of a nonrelativistic intensity, and $\alpha=1.25$ W$^{-1}\times10^{-18}$cm^2 μm^{-2} for the case of a relativistic intensity. We adopt $\alpha=2.8\times10^{-18}$ W^{-1} cm^2 μm^{-2} here for our case. From Eq. (1), one can get an electron emission angle of $\sim3°$ to the normal direction under our experimental conditions. This value is very close to our result.

2. Electron energy spectrum

A typical hot-electron energy spectrum measured in the normal direction is shown in Fig. 3. The laser irradiated an aluminum foil at 45° incidence angle. The 8% prepulse arrived target surface 50 ps earlier than the main pulse. It is obvious that two groups of hot electrons were generated in the interaction. Fitted with the experimental data with Boltzmann distribution, the effective temperatures are 10 and 66 keV, respectively. The lower temperature is consistent with the conventional resonant absorption scaling [21], $T_h=6\times10^{-5}[I\lambda^2(\mathrm{Wcm}^{-2}\ \mu\mathrm{m}^2)]^{0.33}$ keV, which gives 9 keV for the intensity 5×10^{15} W/cm^2. The 66-keV hot temperature is higher than the value given by ponderomotive potential energy scaling [10]. The scaling proposed by Beg *et al.* [28], $T_h=100[I\lambda^2/10^{17}(\mathrm{W\,cm}^{-2}\ \mu\mathrm{m}^2)]^{1/3}$ keV, gives a hot temperature of 32 keV. This temperature value is different from our experimental value. However, taking the differences in the experimental conditions and the temperature measurement techniques into account, the two values are comparable. (K_α x-ray spectra and bremsstrahlung spectra measurement techniques were adopted by Beg *et al.* The self-generated magnetic fields may affect the K_{alpha} measurement technique [29]. Purely collisional interpretations of fast electron transport in K_α emission experiments will underestimate the number and energy of fast electrons [30].)

3. Energy absorption measurement

Hot-electron generation is closely related to laser-plasma coupling processes. We carried out an energy absorption experiment to confirm the dominant energy absorption mechanism. Initially we used two separate calorimeters with 20 mm diameter aperture to measure the scattered laser lights. The spatial distribution of scattered light was obtained by setting the calorimeters at different positions. We found that nearly all of the light was reflected into a small solid angle in the specular direction when laser beam was incident obliquely without prepulses. This implies that short pulses interact with a very thin skin layer less than a laser wavelength. However, the light was scattered into a wide solid angle when a prepulse was introduced. Therefore, the separated calorimeter was replaced by a 4π calorimeter in the later experiments. The 4π calorimeter collected all the scattered light except the back-reflected light, which is only a few percent and thus negligible.

The absorption measurements conducted with 100 μm-thick aluminum foil target for both *p*-polarized and *s*-polarized laser beams are shown in Fig. 4. A prepulse 50 ps before the main beam was introduced. The absolute absorption coefficient could not be obtained because the calorimeter was not calibrated. We can see the reflectivity dependence on incident angle for both *p*- and *s*-polarized irradiation. Similar results have been observed in absorption experiments with picosecond laser-plasma interactions [31,32]. The maximum absorption for a *p*-polarized laser is at a 20° incidence angle. This corresponds to a plasma scale length of $L\sim2\lambda$. These results indicate that the resonance absorption plays an important role in the laser-plasma coupling process. Other processes such as vacuum heating [19,33], etc., may also be responsible for the generation of hot electrons with higher energy.

B. Thin foil experiments

Outgoing hot electrons produced in laser-plasma interactions were ejected from the plasma after overcoming the charge separation potential. On the other hand, the in-going hot electrons in the forward direction will be transported into

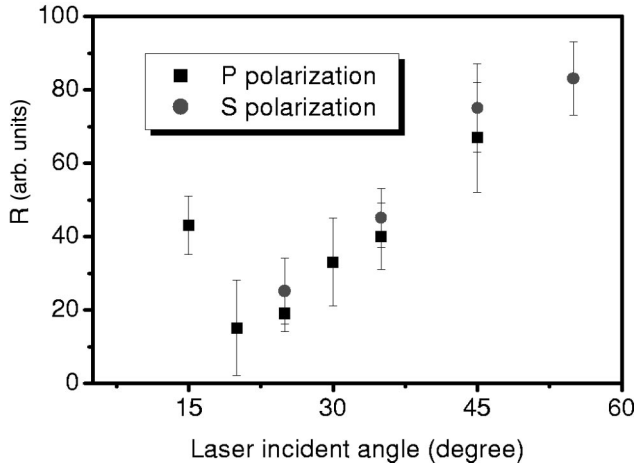

FIG. 4. Angular dependence of the measured reflectance for *p*-polarized beam (square) and *s*-polarized beam (circle) with a prepulse 50 ps before the main beam. Each point is the average of several shots with the statistical error shown as error bar.

the overdense plasma region and cold target region. Hot electrons with higher energies can even pass through the foil target.

We measured the angular distribution of ingoing electrons using radiochromic films with aluminum filter set at the back side of the foil target. Figure 5 shows the angular distributions of the in-going hot electrons with energies greater than 30 keV. The targets were 5-μm-thick aluminum foils. The incident laser intensity was 5×10^{15} W/cm^2. The incident angle was 30° and the light was *p* polarized in these experiments. The dotted line and the dashed line in Fig. 5(a) denote the results obtained with an 8% prepulse 50 ps before the main pulse and without prepulses, respectively. The 0° on *x* axis corresponds the laser propagation direction. Negative angle represents the angle clockwise from the laser propagation direction. From Fig. 5, we can see immediately that, (a) the angular distribution of hot electrons for the case without preplasmas is isotropic; (b) the hot-electron flux for the case with preplasmas is stronger than that without preplasmas; (c) the distribution of hot electrons for the case with preplasmas consists of two components. One is a very broad distribution, which can be regarded as a uniform background. A peak distribution at $-8°$ is superposed on the uniform background. Fitted with a Gaussian distribution (shown as solid line), the full width at half maximum (FWHM) of the peak is 24°, and the maximum emission is at $-8°$. Compared with the outgoing hot electrons, which emit in the normal direction, the ingoing electrons are in the direction close to the laser propagating direction.

The ingoing hot electrons recorded by Radiochromic films have to pass two regions: the plasma region and the cold target region. The physics processes are different for these two regions. In the plasma region, the main effects on hot-electron transport come from the self-generated electric and magnetic fields apart from collisional effects. On the other hand, in the cold target region, the collisions of hot electrons with target ions, bound and free electrons will lead to the direction change and energy loss. We employed a three dimensional (3D) Monte Carlo code to calculate the transport of the energetic electron beam inside an aluminum foil. The foil thickness was chosen to be 5 μm, the same as the foil target used in experiments. An electron source was set to be in the front surface of the foil. The electron number and energy were recorded behind the foil. In the first simulation, electrons with energies of 500, 80, and 30 keV were perpendicularly injected into the foil, respectively. In the second simulation, the electron source with energy of 500 keV was set to be isotropic. We divide the 2π space behind the foil into many smaller annular zones. The differential solid angle for each zone is $2\pi d(\cos\theta)$. Figure 6 shows the angular distribution of electrons passing through the foil. In the Monte Carlo simulations, both the electron energy spectra and spatial distributions were calculated. However, we are more interested in the angular distribution here, so the data shown in Fig. 6, which represents the angular distributions of electrons, were obtained by integrating the whole electron spectra in each annular zone. For the normal incidence in the first simulation, almost all of the 500 keV electrons fall into the 0° annular zone. That is to say, these electrons remain well collimated. However, the angular divergence increases with the reduction of electron energy. Taking 80 keV electrons for example, only 46% of electrons fall into the 26°

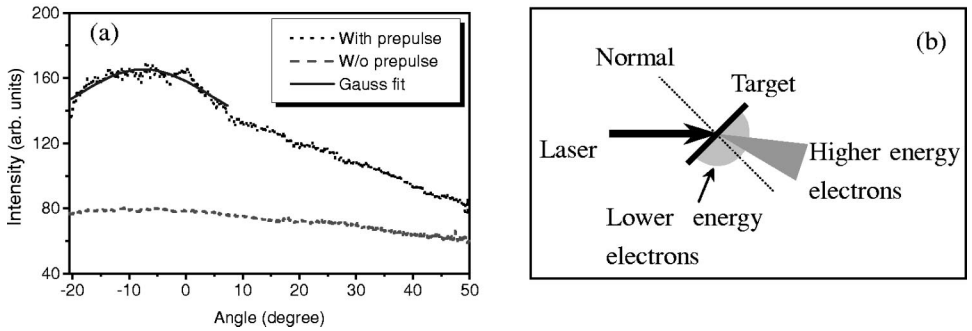

FIG. 5. (a) Angular distribution of ingoing hot electrons with energies greater than 30 keV, measured at the backside of a 5 μm-thick foil target. The dotted line and dashed line are for the case with and without prepulse, respectively. A peak at $-8°$ with 24° FWHM is superposed on a very broad uniform distribution for the case with prepulses. No such peak for the distribution without prepulses. (b) Sketch of the hot-electron emission at the backside of the target for the case with prepulses. Low-energy electrons spread into wide angle as a uniform background of the higher-energy hot electrons.

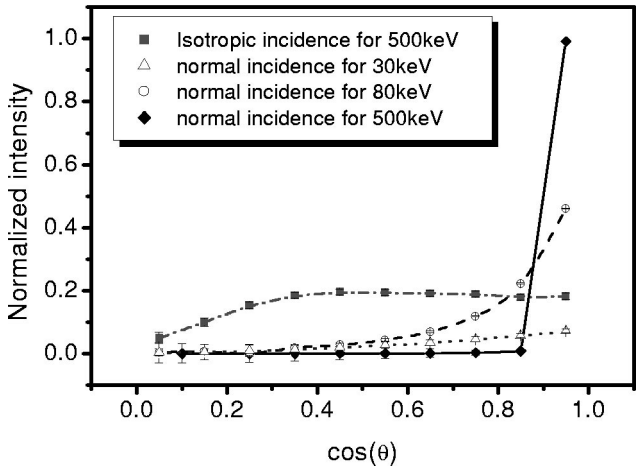

FIG. 6. The theoretical angular distribution of hot electrons recorded behind a 5-μm-thick aluminum foil obtained by 3D Monte Carlo code. The circle is for an isotropic electron source (shown $\times 5$). θ is the angle relative to the normal direction of aluminum foil. For the collimated electron beams perpendicular to the foil, the divergence angles are wider for the lower-energy electrons.

cone angle, shown as the open circles in Fig. 6. For the isotopic input in the second simulation, the distribution remained isotropic within the range of angle $0° \sim 70°$. The number of electrons falling into the range greater than 70° decreases because of their longer path in the target.

The emission direction of hot electrons is different for different acceleration mechanisms. The resonance absorption produces electrons in the direction of electron density gradient, which is observed for the outgoing electrons in our experiments. Ponderomotive potential and wake field mechanisms generate hot electrons along the laser propagation direction. However, they are significant only for higher-laser intensities. No such longitudinal acceleration scheme present for our intensity of 5×10^{15} W/cm^2. Both of the collisional effects and the angular scattering processes in the plasma region and the cold target region are the main reasons for the angular divergence of hot electrons. But these effects cannot explain the collimation of the hot electrons in the laser propagation direction. It is well known that the intense electric fields and magnetic fields exist in laser-plasma interactions. These fields may play important roles in electron transport process into solid targets. J. R. Davies *et al.* considered the transport of hot electrons using a relativistic Fokker-Planck equation. The proposed growth rate of the magnetic field can be written approximately [30] as

$$\frac{\partial B}{\partial t} \sim 3 \times 10^{-2} \frac{\eta f_a}{d} \left(\frac{I}{\lambda} \right)^{2/3} \mathrm{T\,ps^{-1}}, \tag{2}$$

where η is the resistivity in $\Omega \cdot$ m, f_a is the absorption fraction, I is the laser intensity in W/cm^2, d is the focal spot diameter in micro, λ is the laser wavelength in micro, B is the self-generated magnetic field in T. The magnetic field increases to a large magnitude very rapidly. The role of the electric field is to reduce the kinetic energy of hot electrons. On the one hand, the self-generated magnetic fields can collimate the electrons, on the other hand the propagation direction of electron beam can be changed or deflected if the fields are nonsymmetrical distributed. The direction of hot electrons is easily changed by any minor nonsymmetry of magnetic fields due to their light mass. Our previous optical diagnostic experiments using laser probing showed a nonsymmetrical plasma expansion [34]. The deflection of protons due to self-generated magnetic fields was also observed. E. Clark, etc., observed a ring structure of protons, and the ring center deviated about 10° from the target normal in the ultraintense laser-solid interactions [35,36]. The authors believed that the protons were deflected by magnetic fields. Another experiment to study the effects of plasma density scale length on the direction of hot electrons showed that two electron beams were produced, and depending on the structure of the magnetic fields, the two electron beams could change their direction or coalesce together while traversing such fields [37]. These analyses suggest that the hot electrons propagating through the solid target might be bent by the magnetic fields in the interaction region and the overdense region.

The x-ray measurements showed that the prepulses could enhance the emission and energy of hot electrons dramatically [26]. The hot-electron temperature deduced from the x-ray spectrum was about 10 keV for the case without prepulses. When a prepulse was used, the x-ray spectrum presented a double Maxwellian distribution. A group of electrons was accelerated to a much higher energy (66 keV) measured by the electron spectrometer (Fig. 3)

Based on experimental results and theoretical calculation, the angular distribution of in-going hot electrons may be explained as follows. When the in-going hot electrons produced in the laser interactions pass through the plasma region, they are deflected by the self-generated magnetic fields and tend to propagate in the laser propagation direction. The collisional effects in plasma region and in cold material region lead to the energy loss and broaden its angular distribution. The multiple scattering is not very effective for the hot electrons with higher energies, so they remain well directional. However, the hot electrons with lower energies can be steered significantly due to the serious scattering, therefore, they present as a uniform background.

We can see from the above analyses that the ingoing electrons suffer serious scattering and are sensitive to the electromagnetic fields during transport in dense plasma and cold target material. More recently, a collimated proton beam with up to 55 MeV energy was observed in petawatt laser plasma interactions [38]. It is not easy to deflect protons by collisions and electromagnetic fields due to their large mass. Thus, the trajectory of protons approximates a straight line in dense plasma. Furthermore, the efficiency of the energy transfer of protons to nuclear fuel is much higher than that of hot electrons. So protons may become one of competitive candidates as energy carrier in the fast ignitor concept studies.

IV. CONCLUSION

The angular distributions, energy spectrum of hot electrons produced in the interaction of femtosecond laser pulses

with the aluminum plasmas are investigated at a moderate intensity. A collimated jet of hot electrons is observed in the target normal direction. The emission angle of the hot electrons is in agreement with the angular scaling from the canonical momentum conservation. However, the in-going energetic electron beam passing through the foil target is observed to be in the laser propagation direction. This may be the result of the self-generated magnetic fields. The low-energy electrons, which spread into a wider cone angle due to the collisional effect in plasma and target material, present as continuous background. This process is supported by 3D Monte Carlo simulations. The hot temperatures obtained from the electron spectrum and absorption measurement suggest that resonance absorption might be partially responsible for the generation of hot electrons.

ACKNOWLEDGMENTS

This work was supported by the National Natural Foundation of China under Grant Nos. 19825110, 10005014, and 10075075, the National High-Tech ICF program, and the NKBRSF under Grant No. G19999075200.

[1] M. Tabak *et al.*, Phys. Plasmas **1**, 1626 (1994).
[2] K.B. Wharton *et al.*, Phys. Rev. Lett. **81**, 822 (1998).
[3] M.H. Key *et al.*, Phys. Plasmas **5**, 1966 (1998).
[4] S. Bastiani *et al.*, Phys. Rev. E **56**, 7179 (1997).
[5] J. Fuchs *et al.*, Phys. Plasmas **6**, 2569 (1999).
[6] Th. Schlegel *et al.*, Phys. Rev. E **60**, 2209 (1999).
[7] U. Teubner *et al.*, Phys. Rev. E **54**, 4167 (1996).
[8] M. Roch *et al.*, in *Inertial Fusion Sciences and Applications 99*, edited by Christine Labaune, William J. Hogan, and Kazuo A. Tanaka (Elsevier, Paris, 2000).
[9] G. Malka and J.L. Miquel, Phys. Rev. Lett. **77**, 75 (1996).
[10] S.C. Wilks, W.L. Cruer, M. Tabak, A. Loundon, Phys. Rev. Lett. **69**, 1383 (1992).
[11] A.J. Mackinnon *et al.*, Phys. Plasmas **6**, 2185 (1999).
[12] M. Borghesi *et al.*, Phys. Rev. Lett. **80**, 5137 (1998).
[13] M. Tatarakis *et al.*, Phys. Rev. Lett. **81**, 999 (1998).
[14] M. Borghesi *et al.*, Phys. Rev. Lett. **83**, 4309 (1999).
[15] L. Gremillet *et al.*, Phys. Rev. Lett. **83**, 5015 (1999).
[16] P.A. Norreys *et al.*, Phys. Plasmas **6**, 2150 (1999).
[17] H. Ruhl *et al.*, Phys. Rev. Lett. **82**, 743746 (1999).
[18] Y. Sentoku *et al.*, Phys. Plasmas **6**, 2855 (1999).
[19] F. Brunel, Phys. Rev. Lett. **59**, 52 (1987).
[20] D. Gordon *et al.*, Phys. Rev. Lett. **80**, 2133 (1998).
[21] W. L. Cruer, *The physics of Laser Plasma Interactions* (Addison-Wesley, Redwood City, CA, 1988).
[22] E. Lefebvre *et al.*, Phys. Rev. E **55**, 1011 (1997).
[23] A. Pukhov *et al.*, Phys. Plasmas **5**, 1880 (1998).
[24] W. Yu *et al.*, Phys. Rev. Lett. **85**, 570 (2000).
[25] L.M. Chen *et al.*, Sci. China, Ser. A: Math., Phys., Astron. **43**, 1294 (2000).
[26] P. Zhang *et al.*, Phys. Rev. E **57**, R3746 (1998).
[27] L.M. Chen *et al.*, Phys. Rev. E **63**, 036403 (2001).
[28] F.N. Beg *et al.*, Phys. Plasmas **4**, 447 (1997).
[29] A.R. Bell *et al.*, Phys. Rev. E **58**, 2471 (1998).
[30] J.R. Davies *et al.*, Phys. Rev. E **56**, 7193 (1997).
[31] A.G.M. Maaswinkel, K. Eidmann, and R. Sigel, Phys. Rev. Lett. **42**, 1625 (1979).
[32] K.R. Manes *et al.*, Phys. Rev. Lett. **39**, 281 (1977).
[33] P. Gibbon and A.R. Bell, Phys. Rev. Lett. **68**, 1535 (1992).
[34] Li Yutong *et al.*, Sci. China, Ser. A: Math., Phys., Astron. **44**, 98 (2001).
[35] E.L. Clark *et al.*, Phys. Rev. Lett. **85**, 1654 (2000).
[36] E.L. Clark *et al.*, Phys. Rev. Lett. **84**, 670 (2000).
[37] M.I.K. Santala *et al.*, Phys. Rev. Lett. **84**, 1459 (2000).
[38] M.D. Perry, *Science Technology*, LLNL Report No. 25 (2000).